



**HAL**  
open science

# Hydrogen and oxygen on tungsten (110) surface: adsorption, absorption and desorption investigated by density functional theory

Y. Ferro, E.A. Hodille, J. Denis, Z.A. Piazza, M. Ajmalghan

► **To cite this version:**

Y. Ferro, E.A. Hodille, J. Denis, Z.A. Piazza, M. Ajmalghan. Hydrogen and oxygen on tungsten (110) surface: adsorption, absorption and desorption investigated by density functional theory. Nuclear Fusion, 2023, 63 (3), pp.036017. 10.1088/1741-4326/acb0e2 . hal-04049588

**HAL Id: hal-04049588**

**<https://hal.science/hal-04049588v1>**

Submitted on 28 Mar 2023

**HAL** is a multi-disciplinary open access archive for the deposit and dissemination of scientific research documents, whether they are published or not. The documents may come from teaching and research institutions in France or abroad, or from public or private research centers.

L'archive ouverte pluridisciplinaire **HAL**, est destinée au dépôt et à la diffusion de documents scientifiques de niveau recherche, publiés ou non, émanant des établissements d'enseignement et de recherche français ou étrangers, des laboratoires publics ou privés.



Distributed under a Creative Commons Attribution 4.0 International License

# Hydrogen and Oxygen on tungsten (110) surface: adsorption, absorption and desorption investigated by Density Functional Theory

Y. Ferro<sup>1,\*</sup>, E. A. Hodille<sup>2</sup>, J. Denis<sup>1</sup>, Z. A. Piazza<sup>1</sup>, M. Ajmalghan<sup>1</sup>

<sup>1</sup> Aix-Marseille Univ., CNRS, PIIM, F-13013 Marseille

<sup>2</sup> CEA, IRFM, F-13108 Saint Paul Lez Durance, France

## Abstract

In this work we investigated the adsorption of oxygen and the co-adsorption of oxygen and hydrogen on the (110) surface of tungsten by means of Density Functional calculations. The absorption, recombination and release mechanisms of hydrogen across the (110) surface with oxygen are further established at saturation and above saturation of the surface. It is found that hydrogen and oxygen both adsorb preferentially at three-fold sites. The saturation limit was determined to one monolayer in adsorbate. Oxygen is found to lower the binding energy of hydrogen on the surface and to lower the activation barrier for the recombination of molecular hydrogen. Finally, as on the clean surface, oversaturation in adsorbate is shown to lower both activation barriers for hydrogen absorption and for molecular hydrogen recombination on the (110) surface of tungsten.

\* yves.ferro@univ-amu.fr

## 1. Introduction

Tungsten will be used as a plasma facing material in the next generation of fusion reactors like ITER [1, 2]. During interactions between the plasma and the wall, tungsten materials will be irradiated by a high flux of hydrogen isotopes (up to  $10^{24} \text{ m}^{-2}\text{s}^{-1}$ ). These hydrogen isotopes can enter the material and be trapped in it. This is a source of concern from the safety point of view since the amount of tritium is limited inside the vacuum vessel. It is also a source of concern for operating the machine since the recycling flux of molecules/atoms from the wall to the plasma can affect the plasma operations [3].

It follows that many experimental activities are led in laboratories to achieve a full understanding of hydrogen-tungsten interactions and their impact on the operation of the machine [4]. Surface effects were recently shown to play a significant role in absorption and release of hydrogen from tungsten, and models based on Macroscopic Rate Equations (MRE) have emerged [5-10]. As often, these models are based on Density Functional Theory (DFT) data that provide the required activation energies to the MRE models. Some of these DFT works establish the energetics of hydrogen adsorption on the surface of tungsten [10-16], some other provide the energetics of hydrogen penetration into the subsurface [17-20]. All these works consider a clean surface of tungsten in contact with hydrogen.

However, surfaces are exposed to contaminants that may modify these interactions. One contaminant is boron, and the way boron modifies the interaction of hydrogen with the surface was previously investigated by DFT [21]. Another contaminant is oxygen. In fusion devices, oxygen is one of the main impurities of the plasma as observed by ultraviolet spectroscopy measurements in the WEST tokamak [22]. Oxygen has been probed in post-mortem analysis of tungsten-based plasma facing components (PFCs) exposed to plasma operation in WEST [23]. However, oxide films could be eroded by the plasma in the divertor or first wall of a fusion

reactor. But such oxide films are present on laboratory studies due to oxygen affinity toward tungsten, and oxide films might represent an unaccounted difference between laboratory studies and reactor relevant conditions. These differences must be understood to make correct prediction from laboratory experiments to reactor conditions. [24].

Consequently, the main aim of the present paper is to determine how oxygen modifies surface properties regarding adsorption, absorption and desorption of hydrogen's isotopes in tungsten. The literature is rather scarce on this topic, at least from the modelling side. From the experimental point of view, Whitten et al. [25] previously showed that pre-adsorbed oxygen on the surface limits the amount of hydrogen that adsorbs on the W(110) surface; this is consistent with recent experimental results [26]. Above an oxygen coverage of  $\theta_o = 0.35$ , hydrogen adsorption is inhibited. At the same time oxygen decreases the temperature of molecular hydrogen desorption, which means oxygen would lower the activation energy of the recombination process. This point was recently confirmed by Dunand et al. [26]. From the modelling point of view, oxygen adsorption on the (110) surface of tungsten was previously investigated by DFT to establish an ab-initio phase diagram of oxygen on tungsten (110) based on DFT and Monte-Carlo simulations [27]. However, to our knowledge, no DFT investigation was led on the adsorption of both hydrogen and oxygen on a tungsten surface, which is the purpose of the paper.

This work was conducted on the (110) surface because it is the most stable of the low-index surface orientations of tungsten. In addition, the energetics of hydrogen penetration in the sub-surface of tungsten is very similar for the three low-index surfaces (110), (100) and (111) [18]. Finally, it was shown that oversaturation of hydrogen on tungsten surfaces leads quantitatively to the same effects on both the (110) and (100): it lowers the activation barriers for desorption and absorption. As a consequence, the (110) surface was here chosen to determine the impact of oxygen adsorption on the interaction of hydrogen with the surface. In the following, a model

of the (110) surface of tungsten suited for DFT calculations is built. The stable adsorption configurations for all hydrogen and oxygen coverages (enabled by our model) are determined up to saturation in adsorbate of the surface. Over-saturation of the surface is also considered. These DFT data and related mechanisms will be included in the MRE code MHIMS [5, 28] to complete the surface model already developed [8]. It is also planned to include them in the Dynamics of Wall Element (DWE) module [4] to determine the effect of the surface in short-term retention and how it might affect tokamak operations.

In the end, this paper is organized as follows: section 2 provides the details of the model we built and of the numerical parameters we determined to run the DFT calculations. Section 3 provides the stable adsorption sites for oxygen on W (110) and their energetics. Section 4 does the same but considers the co-adsorption of oxygen and hydrogen on W(110). Section 5 deals with the effect of oxygen with regard to the absorption, recombination and release mechanisms of hydrogen on W(110) before a short discussion and conclusion are given in section 6.

## **2. Methodology section**

The calculations were done using the periodic plane-wave implementation of DFT in the Quantum Espresso package [29]. We employ the PBE exchange-correlation functional [30] and the Vanderbilt ultra-soft scalar-relativistic pseudo-potentials (USPP) [31] with non-linear core correction for tungsten and oxygen; 14 valence and semi-core electrons  $5s^2 5p^6 6s^2 5d^4$  were considered for tungsten and 6 valence electrons  $2s^2 2p^4$  were considered for oxygen. Regarding oxygen, there is a known inaccuracy of DFT to deal with its binding energy [32,33]. In agreement with previous studies and considering the oxygen molecule in its triplet ground state (which is the state of lowest energy as it is found in nature), we found the binding energy (BE) at 6.06eV, which reflects a strong over-binding as compared to the experimental value of 5.23 eV [32,34]. This inaccuracy might be improved with the RPBE functional [33] which has been

developed specifically to this end. However, the hydrogen-tungsten system has been massively investigated with the PBE functional during the past 10 to 15 years. As this work comes within the scope of these previous works and deals with hydrogen also, we continue with the PBE functional for the sake of consistency and in order to participate in building a homogenous set of results. The over-binding of molecular oxygen ( $O_2$ ) was corrected in the following way. Firstly, we noted that Wang et al. [32] proposed a constant shift in the formation energy of oxide by -1.36 eV per molecule to correct the error due to the over-binding of  $O_2$  with GGA functional and for correlation effect in the localized  $3d$  orbitals of oxides. But since here we have a metal, we don't have to deal with the correlation effect in the localized  $3d$  orbitals of an oxide. Consequently, we only apply the correction to the binding energy of molecular oxygen, leading to a constant shift of -0.85eV per molecule. Regarding molecular hydrogen, the DFT energy is used as in our previous studies [11,12,17].

The (110) surface of tungsten was modeled by a six-layer slab, keeping the bottom two layers of tungsten atoms frozen to bulk geometry, with a 20 Å vacuum inserted in the Z-direction as in [11,12,17]. The unit-cell parameter was optimized to  $a = 3.187\text{Å}$  [35] and the tungsten (110) surface was model by a  $2 \times 2$  repetition of the *rhombus* unit-cell of total dimension  $a\sqrt{3} \times a\sqrt{3}$  as shown in **Figure 1** (the same was done in our previous publications [11,17]). The resulting top surface displays four tungsten atoms ( $1/4$  for atoms in the corner and  $1/2$  for atoms on the edge of the working-cell), which allows the oxygen and hydrogen coverages  $\theta_O$  and  $\theta_H$  to vary by steps of  $\Delta\theta = 0.25$ . The coverage  $\theta_X = \frac{n_X}{N}$  is defined as the number  $n$  of adsorbed atoms X ( $X = O$  or H) divided by the number  $N$  of substrate tungsten atoms on the top surface. The Brillouin Zone (BZ) was sampled according to a  $11 \times 11 \times 1$  grid of k-points. A broadening of 0.02 Ry (0.27eV) of the electron occupation was employed according to the Marzari-Vanderbilt scheme [36]. Oxygen requires higher energy cutoffs than hydrogen [10,17] for the expansion of the wave-function and the electronic charge density; we used 55 Ry (748eV) and 420 Ry

(5712eV), respectively. With this set of numerical parameters, the adsorption energy is converged below 10 meV for oxygen and hydrogen.

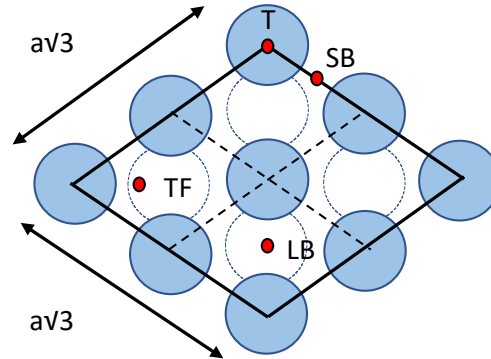


**Figure 1.** Schematic representation of the  $2 \times 2$  rhombus W(110) surface working-cell. The top-surface W atoms are shown in blue, the W atom of the layer below are shown in light-blue. Adsorption sites are indicated by red dots: T (top), TF (three-fold), B (bridge), SB (short-bridge), LB (long-bridge).

Activation energies were determined using the Nudged Elastic Band (NEB) method incorporating the Climbing Image scheme (CI-NEB) [37,38]. As NEB calculations require a large amount of computational resources, looser convergence criteria were selected for NEBs; they are 45 Ry and 360 Ry for the cut-off energies and a  $9 \times 9 \times 1$  grid of k-points for sampling the BZ. With this set of parameters, adsorption energies of oxygen on the (110) surface of tungsten are converged below 20 meV.

A full relaxation of the atomic positions was performed in any case; all the atoms were allowed to relax until the residual force fell below  $10^{-4}$  Ry/Å and the total energy below  $10^{-6}$  Ry. The minimum-energy paths determined with the NEB calculations were considered converged once the norm of the forces orthogonal to the path are less than  $10^{-2}$  eV/Å.

The mass difference between hydrogen and oxygen and between oxygen and tungsten does not allow the approximation that considers the motion of each type of atom are decoupled. As the computational cost of systematically calculating the full phonon frequencies over the entire BZ

would have been intractable, the Zero Point Energy (ZPE) is assumed to compensate between the initial and final states for adsorption, desorption and trapping.

The adsorption energies for oxygen are calculated as follows:

$$E_{ad,O_n} = E_{W_{slab},O_n}^{DFT} - E_{W_{slab}}^{DFT} - \frac{n}{2} E_{O_2}^{exp} \quad (1)$$

where  $n$  is the number of oxygen atoms,  $E_{W_{slab},O_n}^{DFT}$  is the energy value of a given configuration of  $n$  oxygen atoms on the (110) surface of tungsten,  $E_{W_{slab}}^{DFT}$  is the energy of the corresponding bare surface, and  $E_{O_2}^{exp}$  is the energy of molecular oxygen corrected in such a way that the binding energy  $BE = E_{O_2}^{exp} - 2 E_{O_{at}}^{DFT}$  matches with the experimental value of 5.23 eV (it thus consisting in applying a shift of -0.85eV to the DFT value).

The adsorption energy for hydrogen is calculated as:

$$E_{ad,\theta_{O_m},\theta_{H_n}} = E_{W_{slab},O_m,H_n}^{DFT} - E_{W_{slab},O_m}^{DFT} - \frac{n}{2} E_{H_2}^{DFT} \quad (2)$$

As the coverage ratio is increased, the change in adsorption energy of adding an additional oxygen or hydrogen atom upon the most stable configuration is calculated as:

$$E_{ad,O}^{n+1} = E_{W_{slab},O_{n+1}}^{DFT} - E_{W_{slab},O_n}^{DFT} - \frac{1}{2} E_{O_2}^{exp} \quad (3)$$

$$E_{ad,H}^{n+1} = E_{W_{slab},O_m,H_{n+1}}^{DFT} - E_{W_{slab},O_m,H_n}^{DFT} - \frac{1}{2} E_{H_2}^{DFT} \quad (4)$$

### 3. Adsorption of oxygen on the W(110) surface

#### 3.1 – Oxygen on the W(110) surface

##### 3.1.1 - Adsorption and diffusion of oxygen at coverage $\theta_o = 0.25$

One oxygen atom adsorbed on the  $2 \times 2$  rhombus working-cell corresponds to an oxygen coverage of  $\theta_o = 0.25$ . Several adsorption sites were investigated. Among the 3-fold (TF),



long-bridge (LB), short-bridge (SB) and top position (T) displayed in **Figure 1**, only the TF, LB and T position led to geometry that minimizes the energy of the system. The corresponding adsorption energies calculated according to equation 1 and 3 are reported in **Table 1**. The lowest energy adsorption site is found for the TF position.

Additionally, the diffusion of an oxygen atom on top of the surface has been investigated according to the NEB technique. The minimum energy path goes from TF-to-TF sites as shown in **Figure 2**. From the TF site 1 to the TF site 2, oxygen is on top of the activation barrier at the LB site with an energy of 0.17 eV. Consequently, the LB site is not a minimum in energy but most probably a saddle point. From the TF site 2 to the TF site 3, the top of the activation barrier corresponds to the SB site with an activation energy of 0.59 eV.

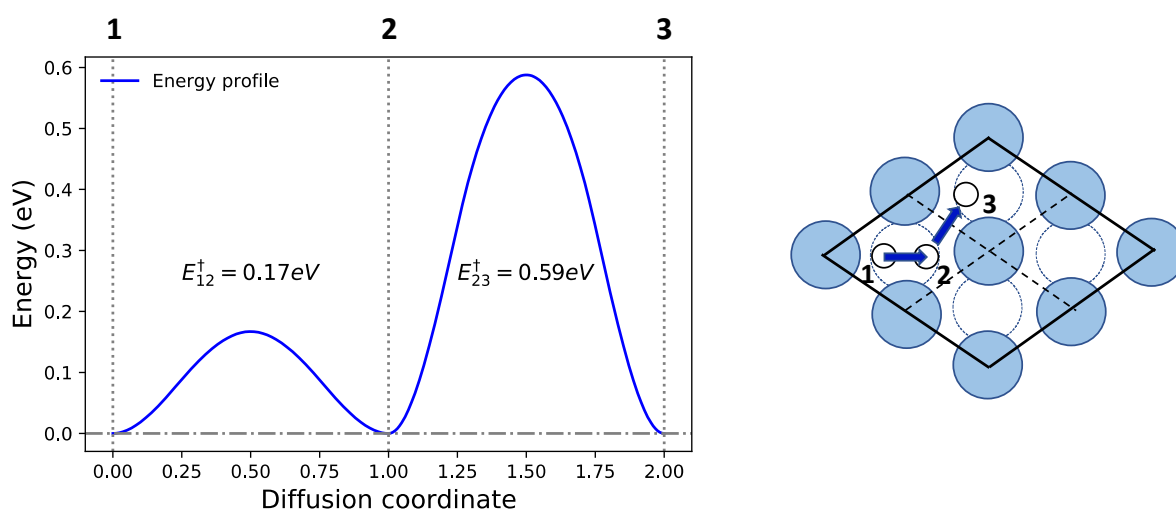


**Figure 2.** Diffusion of oxygen on top of the (110) surface of tungsten at coverage  $\theta_o = 0.25$ . The energy profile is given on the left, while the TF adsorption sites involved are displayed on the right.

Adsorption of oxygen on top of the W(110) surface was previously investigated by DFT in Ref [27] with the PBE functional and using the DFT energy as a reference for the oxygen molecule. The adsorption energies found were -4.16eV (TF), -3.90 (LB) and -3.08 eV (T). This is quite similar to our values if the DFT reference is used for the BE of  $O_2$  as can be seen in **Table 1**.

Experimentally, the O p(2×2) phase has not been observed at  $\theta_o = 0.25$ . Such a coverage however exists and consists in a phases separation between a 2D-gas phase and the O p(2×1) phase of  $\theta_o = 0.50$  [27, 39]. It is however noticeable that the activation barrier for diffusion at coverage  $\theta_o \leq 0.20$  was measured at 0.59 eV [40], which is exactly the energy we here computed.

**Table 1.**

Oxygen adsorption on the (110) surface of tungsten: the adsorption energies  $E_{ad,o_n}$  (eV) and the adsorption energy of adding an additional atom  $E_{ad}^{n+1}$  (eV *per* O atom) are given at all the coverages  $\theta_o$ .  $E_{ad,o_n}^{DFT}$  is the adsorption energy using the binding energy of O<sub>2</sub> computed by DFT for comparison with Ref [27], instead of the experimental value used for  $E_{ad,o_n}$ . <sup>(1)</sup> configuration as labelled in **Figure 3**, <sup>(2)</sup> number of O atoms adsorbed on the surface, <sup>(3)</sup> number of O atoms adsorbed at a tetrahedral site in the sub-surface, <sup>(4)</sup> formation of WO<sub>2</sub> structures above the surface <sup>(5)</sup> adsorption energy of adding one oxygen atom using  $\theta = 1.25$  with 5 *top* as the reference in energy.

$\theta_o$	Site/config	$E_{ad,o_n}$	$E_{ad,o_n}^{DFT}$	$E_{ad,o}^{n+1}$
0.25	TF	-4.56	-4.13	-4.56
	LB	-4.39	-3.96	
	T	-3.51	-3.09	
0.50	<b>a</b> <sup>(1)</sup>	-9.06		-4.50
	<b>b</b> <sup>(1)</sup>	-8.90		
	<b>c</b> <sup>(1)</sup>	-8.37		
	<b>d</b> <sup>(1)</sup>	-8.26		
0.75	-	-13.23		-4.17
1.00	-	-17.07		-3.84
1.25	5 <i>top</i> <sup>(2)</sup>	-15.37		+1.70
	4 <i>top</i> – 1 <i>sub</i> <sup>(3)</sup>	-17.16		-0.04
1.50	WO <sub>2</sub> <i>above</i> <sup>(4)</sup>	-19.89		-4.52 <sup>(5)</sup>

### 3.1.2 - Adsorption and diffusion of oxygen at coverage $\theta = 0.50$

Two oxygen atoms adsorbed on the  $2 \times 2$  *rhombus* working-cell correspond to an oxygen coverage of  $\theta_o = 0.50$ . **Figure 3** displays the four stable configurations we found of placing oxygen at the TF sites, while **Table 1** provides their adsorption energies  $E_{ad,o_n}$  and  $E_{ad}^{n+1}$

computed according to equations 1 and 3, respectively. Configuration **a** has the lowest energy and displays a  $O p(2 \times 1)$  pattern in good agreement with LEED measurements [26, 41, 42].

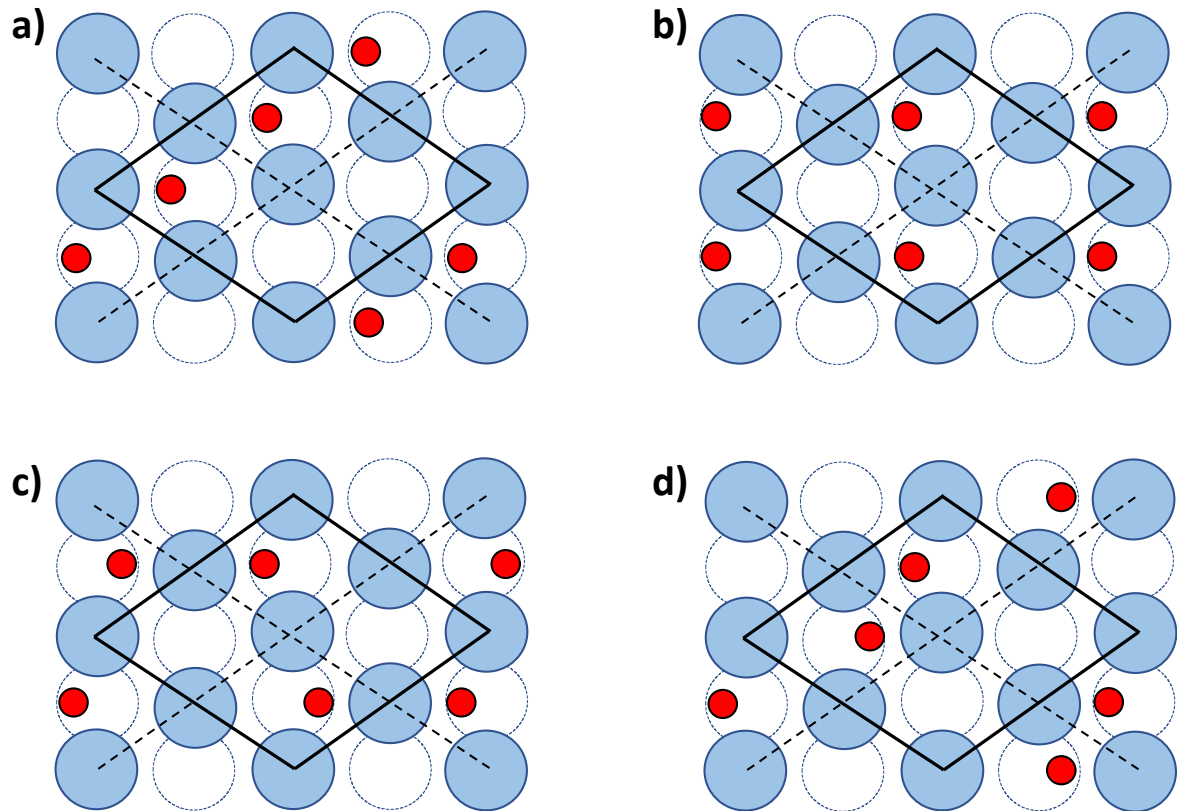


**Figure 3.** Schematic representation of the minimum energy configurations for oxygen at coverage  $\theta_o = 0.50$  on the (110) surface of tungsten.

Additionally, the diffusion of oxygen has been investigated using the NEB technique. One oxygen atom of the working cell was moved while the other one was kept fixed. The path joining site **a** to a symmetrically equivalent site **a** is shown in **Figure 4**. It goes from TF-to-TF sites and involves all **a**, **b**, **c** and **d** sites displayed in **Figure 4**. The main features of **Figure 4** are as follows: (i) the highest activation barrier for oxygen diffusion is from configuration **a** to **c** with a barrier at 0.98eV, (ii) the activation barrier from **d** to **a** is zero (the small bump that can be seen on **Figure 4** is the result of the interpolation procedure), (iii) configuration **d** is consequently metastable and indeed spontaneously relaxes to configuration **a**, and finally (iv)

the second highest barrier is from configuration **a** to **b** in the opposite direction as (i) with an activation barrier at 0.87 eV.

The overall activation barrier of about 1eV is consistent with the previous experimental measurements of Butz and Wagner [43] who determined an activation barrier of  $1.17 \pm 0.10$  eV for  $\theta_o = 0.4 - 0.9$ . Uebing and Gomer [44] also determined an activation barrier of 1.11 eV at  $\theta_o = 0.59$  based on Monte-Carlo simulation with a lattice gas model parametrized such as to reproduce the experimental phase diagram of oxygen on W(110).

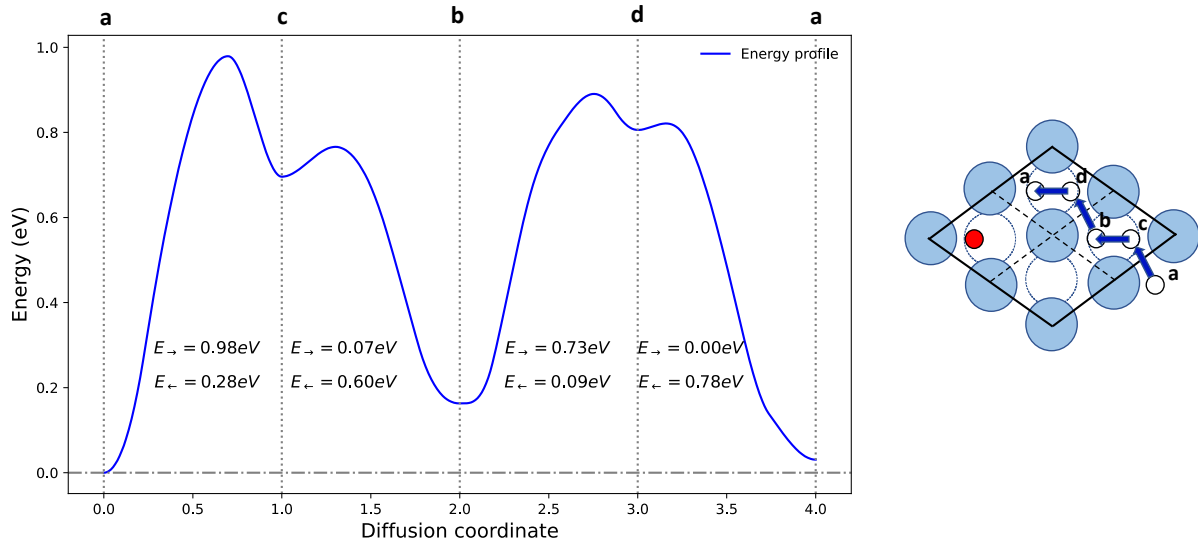


**Figure 4.** Diffusion of oxygen on top of the (110) surface of tungsten at coverage  $\theta_o = 0.50$ . Oxygen moves from sites **a**  $\rightarrow$  **c**  $\rightarrow$  **b**  $\rightarrow$  **d**  $\rightarrow$  **a**. The energy profile is given on the left, while the sites involved and the paths followed are displayed on the right. Activation barriers are given in eV. The small barrier from configuration **d** to **a** is an artefact of the interpolation procedure, it is in fact 0.00 eV.

### 3.1.3 - Adsorption of oxygen on W(110) above $\theta = 0.50$ up to saturation

Three oxygen atoms on the  $2 \times 2$  rhombus working-cell is coverage  $\theta_o = 0.75$ . Only one configuration is obtained; it displays a O p(2 $\times$ 2) pattern and is represented in **Figure 5a**. This pattern is in good agreement with LEED measurements by [41] and [26].

With one additional oxygen atom, a full monolayer of oxygen is completed at coverage  $\theta_o = 1.00$  and the oxygen displays a  $\text{O p}(1 \times 1)$  structure displayed in **Figure 5b**, that was already observed [45,46].

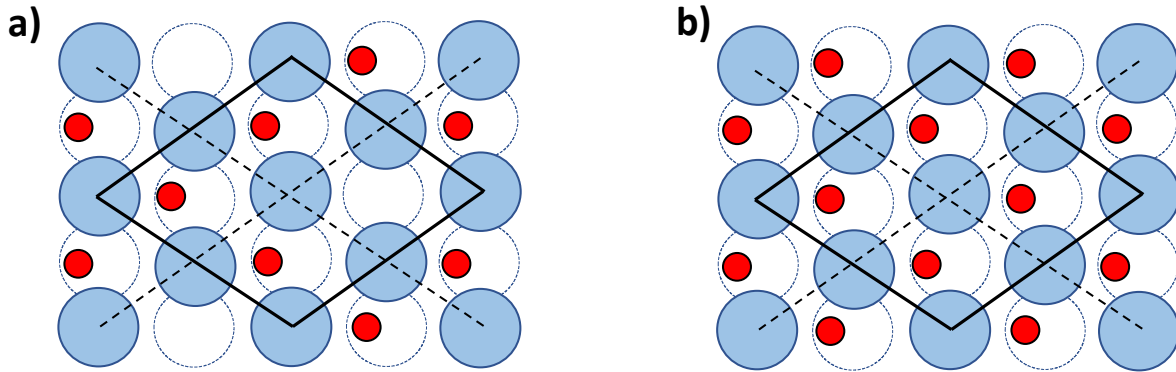


**Figure 5.** Schematic representation of the stable configurations for oxygen at a) coverage  $\theta = 0.75$  and b) coverage  $\theta = 1.00$  on the (110) surface of tungsten.

#### 3.1.4 - Adsorption of oxygen on $W(110)$ above the saturation limit

Subsequent adsorption above one monolayer is disfavored with a positive value of  $E_{ad}^{n+1}$  at  $+1.70\text{eV}$ . Alternatively, the additional oxygen atom above coverage  $\theta_o = 1.00$  may be adsorbed in the subsurface, leading to  $E_{ad}^{n+1}$  at  $-0.04\text{eV}$ . Such a configuration with  $\theta_o = 1.00$  on top and  $\theta_o = 0.25$  in the subsurface is shown in **Figure 6a** and **6b**. It is energetically neutral at 0K, but is entropically disfavored with raising temperature.

When trying to adsorb an additional oxygen atom on the surface to reach coverage  $\theta = 1.50$ , the surface reconstructs and  $\text{WO}_2$  structures emerge as shown in **Figure 6c**, which seems to be energetically favorable as shown in **Table 1**.

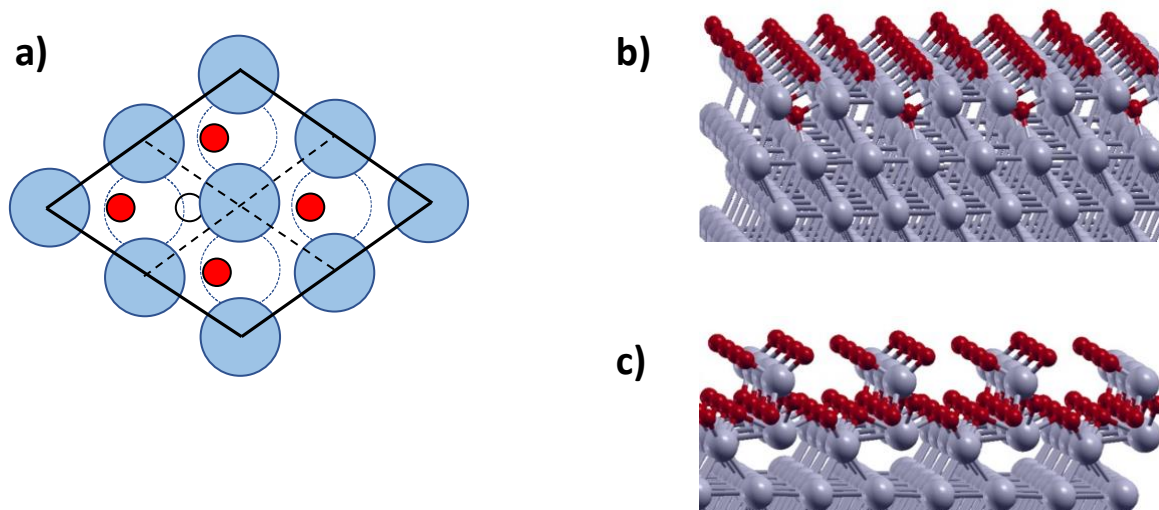


**Figure 6.** a) adsorption of oxygen on W(110) at coverage  $\theta_O = 1.00$  on top with oxygen atoms displayed in red *plus* an additional oxygen atom in the subsurface displays in light-red leading to a total coverage of  $\theta_O = 1.25$ , b) the same, side view. c) Side view of coverage  $\theta_O = 1.50$  with surface reconstruction and  $\text{WO}_2$  protruding units.

### 3.2 – Oxygen in the W(110) subsurface

#### 3.2.1 – Oxygen below the W(110) bare surface

We initially considered the W(110) bare surface and placed an oxygen atom right below in the sub-surface at a tetrahedral site. The geometry optimization spontaneously moved the oxygen atom from below to on top of the surface, and the final position coincides with the TF site described above at coverage  $\theta_O = 0.25$ . We conclude that no oxygen atom adsorbs below the bare W(110) surface.

#### 3.2.2 – Oxygen below the W(110) surface at coverage $\theta_O = 0.75$

We then considered coverage  $\theta_{O,surf} = 0.75$  on top and  $\theta_{O,sub} = 0.25$  in the sub-surface at a tetrahedral site, for a total coverage of  $\theta_O = 1.00$ . This configuration is 3.87eV higher in energy than the configuration with coverage  $\theta_{surf} = 1.00$  on top as described above. A NEB calculation reveals no activation barrier from the configuration  $\theta_{surf} = 0.75$  *plus*  $\theta_{sub} = 0.25$  to the configuration  $\theta_{O,surf} = 1.00$ , and an activation barrier of 3.87eV in the opposite direction. Again, at coverage  $\theta_{O,surf} = 0.75$ , we conclude that no oxygen atom adsorbs below

the surface since no stable position exists. Oxygen prefers to complete one monolayer on top of the surface before it adsorbs in the subsurface.

### 3.2.3 – Oxygen below the W(110) surface at coverage $\theta_O = 1.00$

We further considered the oxygen saturated surface at  $\theta_{O,surf} = 1.00$  and placed an oxygen atom at a tetrahedral site below the surface such as  $\theta_{O,sub} = 0.25$  for a total coverage of  $\theta_O = 1.25$ . As shown in **Table 1**, this configuration is lower in energy by 1.79eV than the configuration with  $\theta_{O,surf} = 1.25$ . It follows that oxygen adsorbs below the surface provided that a monolayer is completed on top. A NEB calculation from coverage  $\theta_{O,surf} = 1.25$  to  $\theta_{O,surf} = 1.00$  plus  $\theta_{O,sub} = 0.25$  yields an activation barrier of 0.66 eV for oxygen to penetrate the surface and of 2.46eV to move backward.

We further consider  $\theta_{O,surf} = 1.00$  and increased the subsurface coverage  $\theta_{O,sub}$  by steps of  $\Delta\theta = 0.25$  up to reach a total coverage of  $\theta_O = 2.00$  with  $\theta_{O,surf} = 1.00$  plus  $\theta_{O,sub} = 1.00$ . In the end, we computed some additional points on the way to coverage  $\theta_O = 3.00$  such that  $\theta_{surf} = 1.00$  and  $\theta_{O,sub} = 2.00$ . These results are plotted in **Figure 7**.

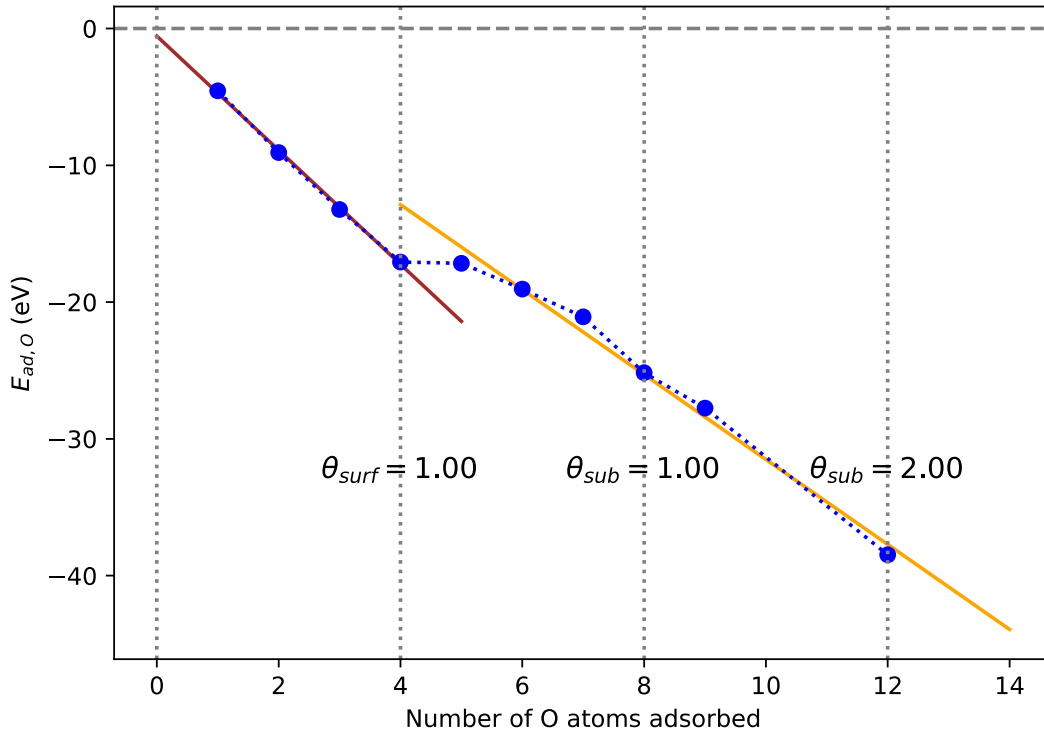


**Figure 7:** Adsorption energy versus the number of oxygen atoms adsorbed on the surface. From  $\theta_o = 0$  to 1; adsorption takes place on the surface. Above  $\theta_o = 1$ , oxygen adsorbs in the subsurface at tetrahedral site between the surface layer and the layer just below.

The global trend is as follows: adsorption of oxygen on the surface results in a monotonous decrease in adsorption energy of -4.17 eV per atom, up to reach saturation in oxygen of the (110) surface of tungsten – 1 ML of oxygen, 4 atoms in the present case. Above saturation, oxygen adsorbs in the sub-surface at tetrahedral sites. The absorption energy monotonically decreases with a slope of -3.11 eV (plotted in orange on the figure below). When reaching the configuration corresponding to 1 ML on top and 2 ML in the sub-surface; a complete  $WO_2$  layer is formed as shown in **Figure 8**. This  $WO_2$  layer is weakly bonded to the rest of the (110) surface at coverage  $\theta = 1.00$ : we computed an interaction energy of only -43 meV, indicating this  $WO_2$  layer could be easily removed from the surface. The  $W_{surf}-W_{layer}$  distance between a tungsten atom of the  $WO_2$  layer and those of the surface is  $5.67\text{\AA}$ . This is large as compared to



the interlayer distance of the (110) planes in tungsten at 2.26 Å. This is also consistent with a weak interaction between the WO<sub>2</sub> layer and the surface.

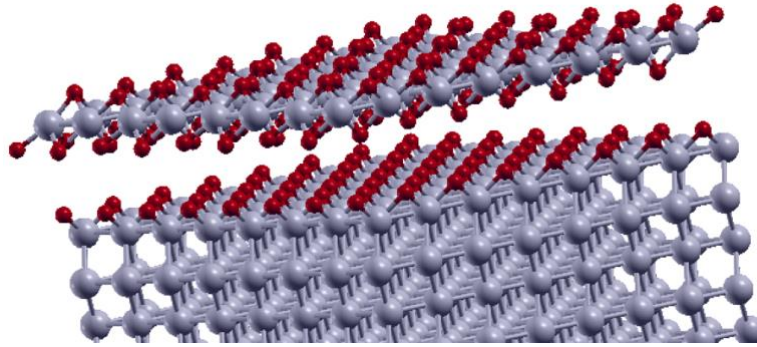


**Figure 8** : WO<sub>2</sub> layer on top of the (110) surface of tungsten at coverage  $\theta = 1.00$ .

### 3.3 – Oxygen and the W(110) surface : summary

The present study reveals that the TF site is the most stable site for adsorption of oxygen on (110) surface of tungsten. The adsorption energy is at -4.56 eV at  $\theta_O = 0.25$  if using the experimental value of molecular oxygen for the BE. The mean value of the adsorption energy is around -4.17 eV per oxygen atom up to saturation of the surface. These are quite strong adsorption energies consistent with the fact that experimentally, tungsten surface needs high temperatures around 1900K to be reduced and cleaned from any traces of oxygen [47].

Regarding the activation energy of oxygen diffusion on the surface, it goes increasing with increasing coverage. This is consistent with experimental observation [44]. When perpendicular to the surface, we were able to find a route to adsorbed oxygen below the surface. Up to saturation in oxygen of the surface, this route has a high cost in energy and could be unlikely. Above saturation, we were able to find an activation barrier of 0.66eV. However, as  $E_{ad}^{n+1}$  at +1.70eV for reaching coverage 1.25, diffusion perpendicular to the surface starting from  $\theta_O = 1.25$  would be unlikely too. In the end, the way oxygen penetrates the surface remains unclear

and could proceed through defect or phase transformation. Nevertheless, if such a route exists, WO<sub>2</sub> layers could form, and tungsten could be delaminated upon oxygen adsorption.

In the remainder of this work, we focus on the surface and investigated the adsorption of hydrogen on top of the (110) surface of tungsten at different coverage in oxygen, with the main aim to determine the impact of oxygen on the adsorption of hydrogen.

#### **4. Adsorption of oxygen and hydrogen on W(110)**

##### *4.1 – Hydrogen adsorption on the W(110) surface with oxygen at $\theta_O = 0.00$*

We previously considered the (110) surface of tungsten free of any oxygen atom at  $\theta_O = 0.00$  and adsorbed hydrogen on top of it [11,12]. The corresponding adsorption energies are reported in **Table 2**. Hydrogen also occupies the TF sites as oxygen does. Saturation in hydrogen of the W(110) surface occurs at  $\theta_H = 1.00$  corresponding to one monolayer of hydrogen as we found with oxygen.

In addition to which we previously did, in the present work we investigate the diffusion property of a single hydrogen atom on top of the (110) surface of tungsten at coverages  $\theta_H = 0.25$  and  $\theta_O = 0.00$ . The path is the same as the one shown in **Figure 2** for oxygen, but the height of the activation barriers is different: from TF1 to TF2 the barrier is the lowest at 0.09eV, while from TF2 to TF3 the activation barrier is not larger than 0.20eV. This result highlights the ability of hydrogen to move on the W(110) surface.

**Table 2**

Hydrogen and oxygen adsorption on the W(110) surface: the adsorption energies  $E_{ad,O_m,H_n}$  (eV) and the adsorption energy of adding an additional atom  $E_{ad,H}^{n+1}$  (eV *per* H atom). (a), (b), (c) and (d) refer to the configurations shown in **Figure 9**. (top) adsorption of hydrogen right on top of oxygen atoms to form OH groups. (av) mean adsorption energy per H atom.

$\theta_O$	$\theta_H$	$E_{ad,\theta_{O_m},\theta_{H_n}}$	$E_{ad,H}^{n+1}$
0.00	0.25	-0.73	-0.73
	0.50	-1.47	-0.75
	0.75	-2.17	-0.70
	1.00	-2.80	-0.63
0.25	0.25	-0.64 <sup>(a)</sup>	-0.64
		-0.56 <sup>(b)</sup>	
		+0.66 <sup>(top)</sup>	
	0.50	-1.29 <sup>(c)</sup>	-0.65
	0.75	-1.89	-0.60
	1.00	-2.32	+0.11
0.50	0.25	-0.47	-0.47
	0.50	-0.95	-0.49
	0.75	-0.68	+0.28
	1.00	-0.39	+0.29
0.75	0.25	-0.36	-0.36
1.00	1.00	+1.73 <sup>(top)</sup>	+0.43 <sup>(av)</sup>

#### 4.2 – Hydrogen adsorption on the W(110) surface with oxygen at $\theta_O = 0.25$

We considered the lowest energy configuration for oxygen at coverage  $\theta_O = 0.25$  (TF site) and adsorbed hydrogen on top of the tungsten surface at various coverages in hydrogen  $\theta_H$ . The lowest energy configurations are represented in **Figure 9** and the corresponding adsorption energies are reported in **Table 2**. The adsorption energy *per* H atom  $E_{ad,H}^{n+1}$  is higher than on the clean surface ( $\theta_O = 0.00$ ) by around 0.1 eV, indicating hydrogen is less bonded to the surface when oxygen is present.

The maximum coverage in hydrogen of the surface is reached at  $\theta_H = 0.75$  for a total coverage in hydrogen *plus* oxygen of one monolayer at  $\theta = 1.00$ , which is consistent with experiment Ref [25]. For  $\theta_H = 1.00$ , the total coverage is  $\theta = 1.25$ , and the adsorption energy  $E_{ad,H}^{n+1}$  becomes positive making further adsorption of hydrogen unfavorable above one monolayer in adsorbate.

Regarding the pattern of the adsorbate, it is noticeable that the most stable configuration is the same whatever the adsorbate is (H, O or H+O) at a given total coverage.

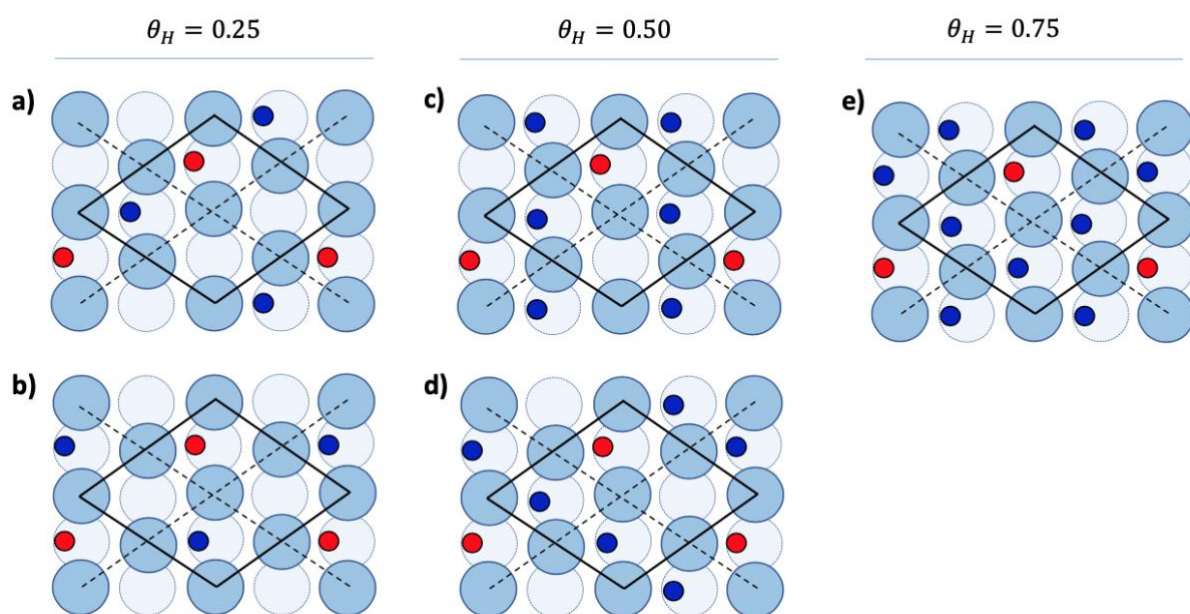


**Figure 9** : lowest energy configurations for various coverage in hydrogen  $\theta_H$  W(110) at coverage in oxygen  $\theta_O = 0.25$ .

We probed the viability of hydroxyl (OH) groups on the surface and placed hydrogen directly above oxygen atoms. The resulting adsorption energy is positive at +0.66eV, which means no hydroxyl group forms on the surface at this coverage in oxygen. This is corroborated by experimental observations too [25].

In the end, the diffusion properties of hydrogen were investigated using the NEB technique at  $\theta_H = 0.25$  and  $\theta_O = 0.25$ . The highest activation barrier was found at 0.42 eV, which means oxygen slows down the diffusion process of hydrogen on the surface.

#### 4.3 – Hydrogen adsorption on the W(110) surface with oxygen at $\theta_O = 0.50$ and above.

**Figure 10** displays the most stable configurations hydrogen adopts on the surface at  $\theta_O = 0.50$  and  $\theta_O = 0.75$  while **Table 2** reports the energetics of each configuration. At  $\theta_O = 1.00$ , no hydrogen adsorbs on the surface. An attempt to form hydroxyl OH groups by placing hydrogen right on top of the oxygen atoms led to a positive adsorption energy of +1.73eV (+0.43eV/H atom), again demonstrating that no OH group form on the surface.

As previously, saturation of the surface is reached for a total coverage in adsorbate of  $\theta = 1.00$ , and the most stable configurations are the same whatever is the adsorbate (H, O or H+O) at a given total coverage. The conclusion is that the same adsorption sites are available on the surface for oxygen and hydrogen, and once hydrogen (respectively oxygen) is adsorbed, oxygen (respectively hydrogen) cannot be adsorbed anymore. This is again in good agreement with the experimental work of Whitten and Gomer [25].

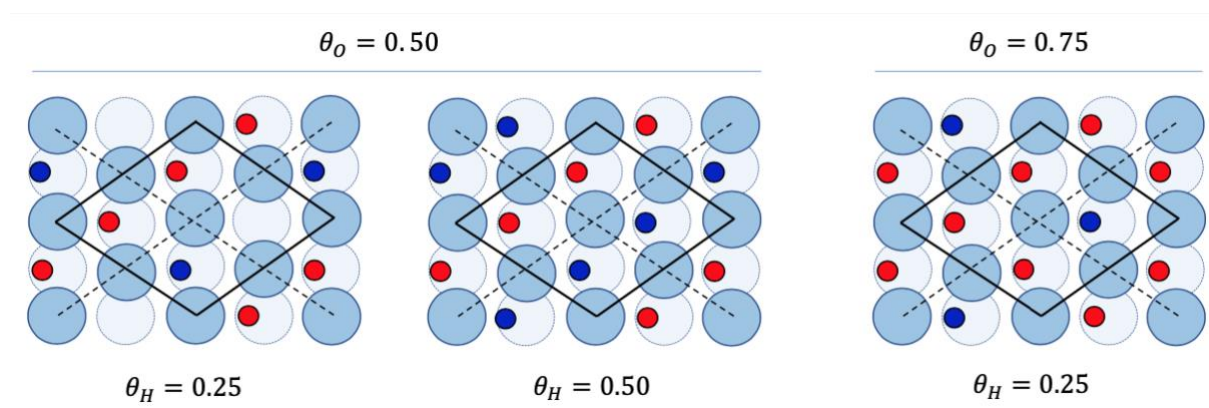


**Figure 10** : lowest energy configurations for various coverage in hydrogen  $\theta_H$  on the (110) surface of tungsten at coverage in oxygen  $\theta_O = 0.50$ .

#### 4.4 – Hydrogen adsorption on the W(110) surface with oxygen: summary and comments.

Finally, the full energetics of oxygen *plus* hydrogen adsorption on top of the (110) surface of tungsten is displayed in **Figure 11**. The adsorption energy for hydrogen increases as the oxygen coverage of the surface increases, making hydrogen less bonded to the surface. This is in good agreement with Ref [25]. From  $\theta_O = 0.00$  to  $\theta_O = 0.25$ , the loss in binding energy to the surface amounts 0.1eV. From  $\theta_O = 0.25$  to  $\theta_O = 0.50$  it is 0.2 eV, and from  $\theta_O = 0.50$  to  $\theta_O = 0.75$ , it is 0.1eV again.

The reason for this trend is analyzed below in terms of charge following a population analysis. There is no unique way to associate electrons to a given atom, and here we performed a population analysis according to the Löwdin definition [48]. The net charges on the atoms (difference between the electronic charge provided by the Löwdin population analysis and the electronic charge of the isolated atom) and the geometry of adsorption are reported in **Table 3** for four different coverages in adsorbate of the W(110) surface. In each, the coverage in hydrogen is constant at  $\theta_H = 0.25$ , while the number of oxygen atom on the surface increases from  $\theta_O = 0.00$  to  $\theta_O = 0.75$ .

The net charge on hydrogen remains the same whatever the coverage in oxygen. A charge transfer is observed from tungsten to oxygen on the surface. This charge transfer from the tungsten atom of the TF site increases as the number of oxygen atoms increases on the surface (**Table 3**). **Figure 12** also report the charge density difference between the charge density of the surface minus the charge density of the isolated atoms. It is plotted in  $e/\text{\AA}^3$  in the  $[\bar{1}10]$  plane perpendicular to the [110] plane of the tungsten surface at  $\theta_O = 0.00$  and  $\theta_O = 0.50$ . The charge density is reduced around the hydrogen atom at  $\theta_O = 0.50$  as compared to  $\theta_O = 0.00$ , making hydrogen less bonded to the surface (the same is observed for  $\theta_O = 0.25$  and  $\theta_O = 0.75$  not shown). This charge density reduction is consistent with the charge transfer from tungsten to oxygen reported in **Table 3**. At the same time hydrogen is less bonded to the surface, and the distance from hydrogen to the (110) surface increases (**Table 3**). Such an effect was

already observed for boron which, when co-adsorbed with hydrogen on the (100) surface of tungsten, reduces the electronic density around the adsorbed H atom, making H less bonded to the surface [21].

Because the adsorption energy increases with increasing coverage in oxygen, at  $\theta_O = 0.50$ , the adsorption energy of hydrogen is higher than -0.5 eV. This would explain why no hydrogen adsorbs above this oxygen coverage on W(110) [25] at room temperature. In case oxygen is pre-adsorbed, there are less available adsorption sites left for hydrogen since the maximum coverage is one monolayer in adsorbate. This is in good agreement with Ref [26] who show by TDS that the total amount of hydrogen decreases with increasing coverage in oxygen.

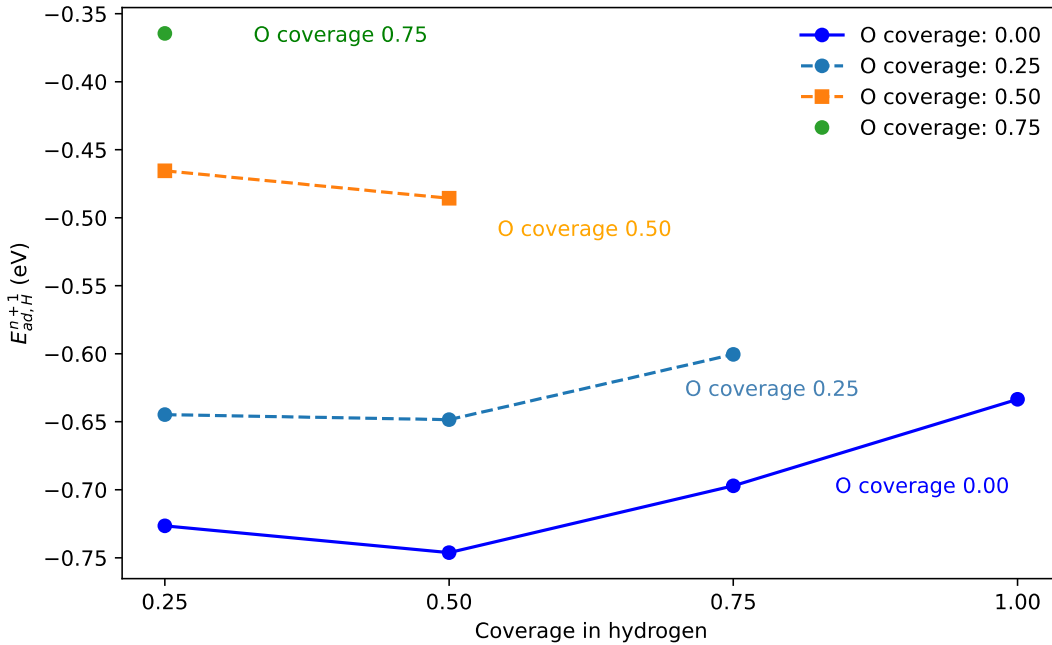


**Figure 11** : Full energetics of the oxygen *plus* hydrogen coverage on the W(110):  $E_{ad,H}^{n+1}$  in eV plotted versus the coverage in hydrogen  $\theta_H$ .

**Table 3**

Net charges (difference between the electronic charge provided by the Löwdin population analysis and the electronic charge of the isolated atom) and geometry of adsorption for one hydrogen atom ( $\theta_H = 0.25$ ) adsorbed on the W(110) surface at various oxygen coverages from  $\theta_O = 0.00$  to  $\theta_O = 0.75$ .  $q_H$  is the net charge (in  $e$ ) on H,  $\bar{q}_W$  is the average net charge (in  $e$ ) of the three tungsten atoms of the TF sites involved in hydrogen adsorption,  $\bar{q}_O$  is the average net charge (in  $e$ ) born by the oxygen atoms. The distance from hydrogen to the plane of the (110)



surface and the average distance of hydrogen to the tungsten atoms of the TF site are also provided in Å.

$\theta_o$	$q_H$	$\bar{q}_W$	$\bar{q}_O$	$d_{H-plane}$	$\bar{d}_{H-W}$
0.00	0.06	0.01	-	1.058	2.007
0.25	0.05	0.08	-0.36	1.033	2.020
0.50	0.06	0.18	-0.36	1.066	2.024
0.75	0.03	0.31	-0.35	1.139	2.025

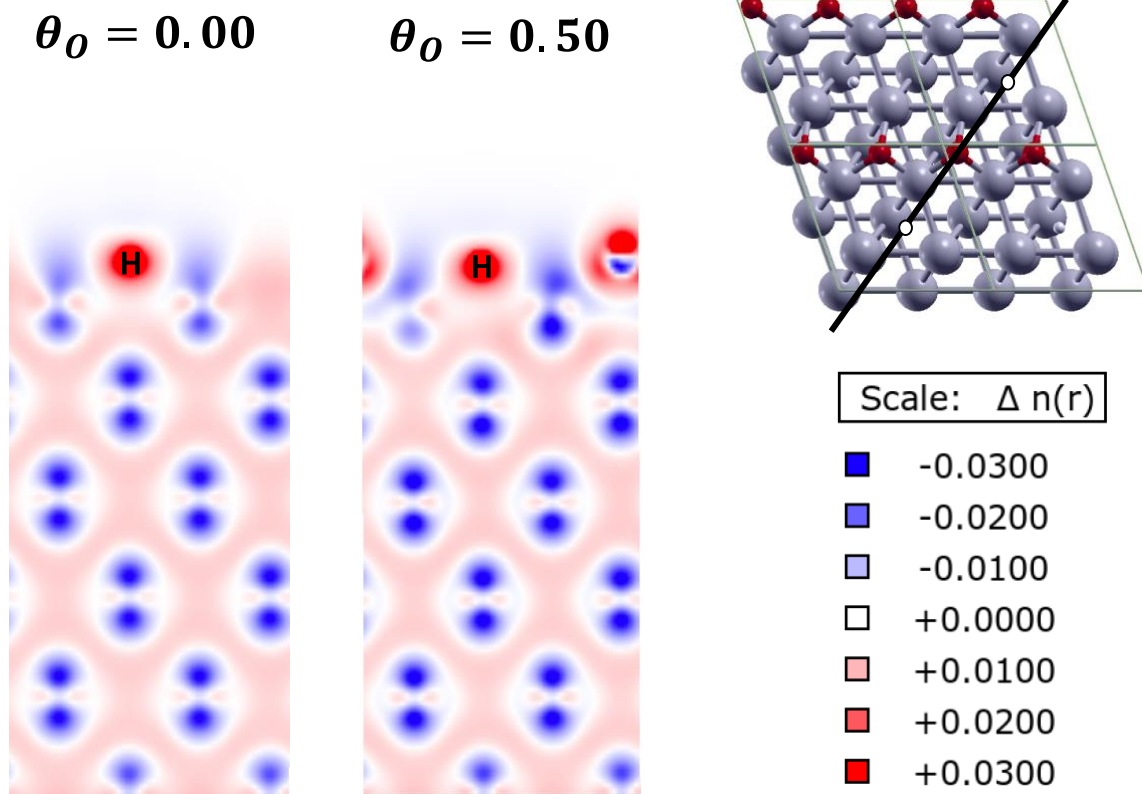


**Figure 12** : Charge density difference ( $e/\text{\AA}^3$ ) plotted in the  $[\bar{1}10]$  plane perpendicular to the  $[110]$  plane of the tungsten surface. The charge density is plotted for one hydrogen atom ( $\theta_H = 0.25$ ) at  $\theta_o = 0.00$  and  $\theta_o = 0.50$  for a charge difference ranging from  $-0.03$  to  $0.03 e/\text{\AA}^3$ . The  $[\bar{1}10]$  plane is shown as a black line on the top right of the Figure where the hydrogen atoms are shown as white dots.

## 5. Hydrogen absorption and desorption through the W(110) surface at various oxygen coverages

### 5.1 – Absorption and desorption mechanisms.



The full energy paths were determined for hydrogen absorption from the gas phase to the bulk (and conversely). Two coverages in oxygen were considered:  $\theta_O = 0.25$  to  $\theta_O = 0.50$ . Indeed, the clean surface at  $\theta_O = 0.00$  was previously investigated by us [17], and  $\theta_O = 0.75$  was shown non-reactive to hydrogen when exposed to a  $H_2/D_2$  atmosphere [25,26] since no adsorption is observed. Regarding the coverage in hydrogen, it was chosen such as to be consistent with saturation in adsorbate of the surface and oversaturation as in [17]. This led us to consider the three different cases described below.

*First case:* at  $\theta_O = 0.50$ , a hydrogen molecule  $H_2$  is dragged from the gas phase to the W(110) surface where it dissociates. Then a hydrogen atom is further dragged to a tetrahedral (Td) interstitial site into the bulk. The hydrogen coverage is chosen such that the surface is saturated in adsorbate when  $H_2$  is dissociated. For that reason, this system will be referred to as  $\theta_O = 0.50$  and  $\theta_H = 0.50$  (shortly  $\theta_{O/H} = 0.50/0.50$ ). The evolution of the surface coverage in hydrogen along the path is as follows:  $\theta_H = 0.00$  when hydrogen is in the gas phase,  $\theta_H = 0.50$  when  $H_2$  is dissociated on the surface, and finally  $\theta_H = 0.25$  when a hydrogen atom is into the bulk at an interstitial site.

*Second case:* The same is done at  $\theta_O = 0.25$ . Again, the surface is saturated when the hydrogen molecule is on the surface, and this case will be referred to as  $\theta_O = 0.25$  and  $\theta_H = 0.75$  ( $\theta_{O/H} = 0.25/0.75$ ). The evolution of hydrogen surface coverage is from  $\theta_H = 0.25$  when hydrogen is in the gas phase, to  $\theta_H = 0.50$  when a hydrogen atom is at an interstitial site into the bulk.

Both these cases will be referred to as *saturation*.

*Third case:* it corresponds to  $\theta_O = 0.25$  and  $\theta_H = 0.75$  on the surface *plus* one hydrogen atom at an interstitial site below the surface. As a consequence, when the interstitial hydrogen atom reaches the (110) surface, it is over-saturated and the hydrogen coverage raised to  $\theta_H = 1.00$ .

This case will correspondingly be referred to as  $\theta_O = 0.25$  and  $\theta_H = 1.00$  ( $\theta_{O/H} = 0.25/1.00$ ) and named *oversaturation*. It is intended to mimic the situation where the surface is already saturated in adsorbate, and implanted hydrogen atoms diffuse up to the surface where they recombine and desorb. *Oversaturation* was already shown to dramatically lower the activation barrier for adsorption and desorption on the clean W(110) and W(100) surfaces [17]. Here we will determine the effect of *oversaturation* in the presence of oxygen. The evolution of the surface coverage at *oversaturation* ( $\theta_{O/H} = 0.25/1.00$ ) is as follows: coverage of  $\theta_H = 0.50$  when hydrogen is in the gas phase,  $\theta_H = 1.00$  when dissociated on the surface, and finally  $\theta_H = 0.75$  when a hydrogen atom is at an interstitial site into the bulk.

### 5.2 – Energy profiles at surface saturation and over.

The corresponding energy paths are displayed in **Figure 13**. In abscissa are numbered the interstitial sites located at tetrahedral positions (Td) as in Ref [17]. They are numbered from zero when located on the surface to eight (Td<sub>8</sub>) at 5.6Å below the surface. Location -1 is for hydrogen into the gas phase at 10 Å away from the surface.

Each curve is plotted with a reference in energy set at zero when hydrogen is in the bulk at interstitial site Td<sub>4</sub>. All the activation barriers are reported in **Table 4** in the forward (from the surface to the bulk) and backward (reverse) direction.

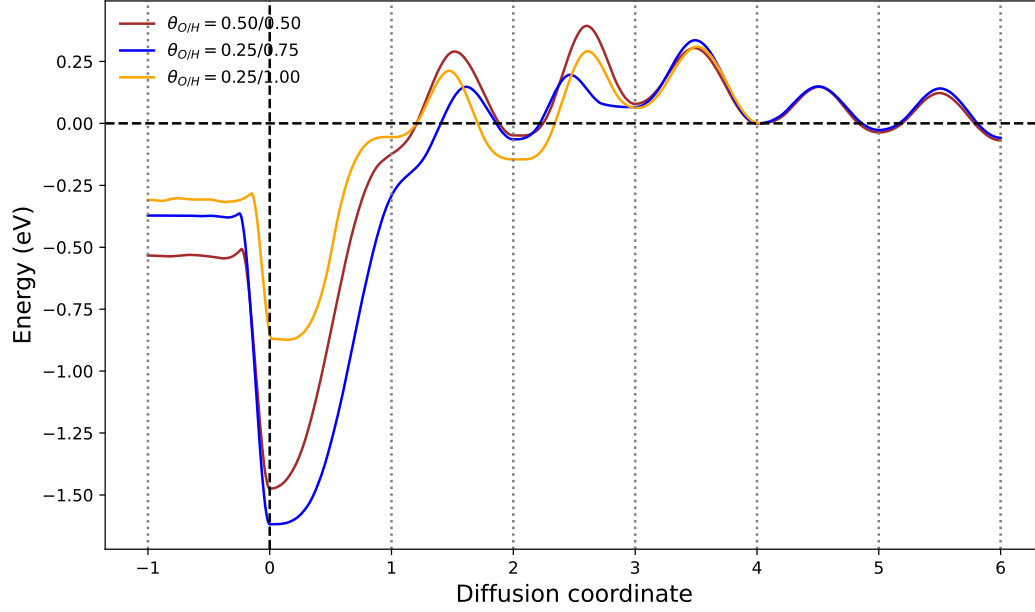


**Figure 13:** Diffusion energy paths for the dissociation of a hydrogen molecule on (110) tungsten surface and atomic hydrogen absorption across the tungsten sub-surface are plotted for three different coverages. Three cases are considered,  $\theta_{O/H} = 0.50/0.50$  and  $\theta_{O/H} = 0.25/0.75$  correspond to *saturation* of the surface, and  $\theta_{O/H} = 0.25/1.00$  corresponds to *oversaturation* in adsorbate of W(110). Diffusion coordinate in abscissa provides the  $j$  position of the  $Td_j$  interstitial site considered. Coordinated 0 and -1 corresponds to the surface and the gas phase, respectively. The reference energy for all curves was set to zero for H atom at  $Td_4$

**Table 4:** Activation barriers in eV for the penetration of a hydrogen atom across the (110) tungsten surface. *Saturation* in adsorbate of the surface and *oversaturation* are considered. The coverages in oxygen are  $\theta_O = 0.25$  and  $\theta_O = 0.50$ . Also activation barriers (eV) for the penetration of hydrogen across the (110) clean surface of tungsten are reported from [17].

Site	Saturation						Over-saturation			
	$\theta_{O/H} = 0.50/0.50$		$\theta_{O/H} = 0.25/0.75$		$\theta_H = 1.00$ [17]		$\theta_{O/H} = 0.25/1.00$		$\theta_H = 1.25$ [17]	
	<i>forward</i>	<i>backward</i>	<i>forward</i>	<i>backward</i>	<i>forward</i>	<i>backward</i>	<i>forward</i>	<i>backward</i>	<i>forward</i>	<i>backward</i>
$H_2 \rightarrow Surf$	0.03	<b>0.97</b>	0.01	<b>1.25</b>	0.04	<b>1.35</b>	0.03	<b>0.59</b>	0.11	<b>0.80</b>
$Surf \rightarrow Td_2$	<b>1.77</b>	0.34	<b>1.76</b>	0.21	<b>1.75</b>	0.20	<b>1.08</b>	0.36	<b>0.90</b>	0.11
$Td_2 \rightarrow Td_3$	0.44	0.32	0.26	0.13	0.09	0.26	0.45	0.23	0.07	0.90
$Td_3 \rightarrow Td_4$	0.23	0.30	0.27	0.34	0.37	0.27	0.25	0.31	0.11	0.18
$Td_4 \rightarrow Td_5$	0.15	0.18	0.15	0.18	0.19	0.14	-	-	0.06	0.17
$Td_5 \rightarrow Td_6$	0.16	0.19	0.17	0.20	0.21	0.18	-	-	0.33	0.27
$Td_6 \rightarrow Td_7$	0.25	0.25	0.24	0.23	-	-	-	-	0.20	0.16
$Td_7 \rightarrow Td_8$	0.20	0.17	0.20	0.18	-	-	-	-	0.21	0.19

The common features to all three plots are the following: (i) the activation barrier for H<sub>2</sub> dissociation on W(110) is negligible, and (ii) there is no minimum in energy for H at the Td<sub>1</sub> position; hydrogen directly diffuses from the surface to Td<sub>2</sub>. Both these features are common with previous results for hydrogen on the clean (110) tungsten surface at  $\theta_O = 0.00$  [17] also reported in **Table 4**. In addition (iii) all curves are superimposed starting from Td<sub>3</sub>, indicating that below Td<sub>3</sub> the impact of oxygen and hydrogen adsorption on top is negligible, and (iv) the activation barriers for diffusion tend to their values in the bulk at 0.20 eV starting from Td<sub>4</sub> (2.86Å): below this point, bulk properties are recovered (the solution energy of H in the bulk is fully recovered starting from Td<sub>6</sub>). This feature is also common with the clean surface.

The three cases also exhibit specific features which are discussed and compared below with results on the clean surface in the case of surface *saturation* ( $\theta_{O/H} = 0.50/0.50$ ,  $\theta_{O/H} = 0.25/0.75$  and  $\theta_H = 1.00$ ) [17] and *oversaturation* ( $\theta_{O/H} = 0.25/1.00$  and  $\theta_H = 1.00$ ) [17].

The activation barrier for hydrogen absorption into the bulk (Td<sub>0</sub> to Td<sub>2</sub>) is 1.77 – 1.76 eV as on the clean surface 1.75eV (**Table 4**); this is the rate-limiting step of the absorption mechanism. In the backward direction, the activation barrier is from 0.21eV to 0.36eV, similar to diffusion into the bulk. However, at *oversaturation*, the activation barrier for absorption is dramatically reduced from 1.76eV ( $\theta_{O/H} = 0.25/0.75$ ) to 1.08 eV ( $\theta_{O/H} = 0.25/1.00$ ). In the same way, the activation barrier for molecular hydrogen recombination is also dramatically reduced from 1.25 eV ( $\theta_{O/H} = 0.25/0.75$ ) to 0.59 eV ( $\theta_{O/H} = 0.25/1.00$ ). This *oversaturation* effect is similar to what was established on the clean surface [17] (**Table 4**).

The specific effect of oxygen manifests itself at *saturation*: from  $\theta_O = 0.00$  to  $\theta_O = 0.25$ , the activation barrier for molecular recombination drops by 0.1 V from  $E_{clean}^{\ddagger} = 1.35$  eV to  $E_{025}^{\ddagger} =$

1.25 eV. From  $\theta_o = 0.25$  to  $\theta_o = 0.50$ , it drops by 0.27 eV from  $E_{O=0.25}^\ddagger = 1.25$  eV to  $E_{O=0.50}^\ddagger = 0.97$  eV. This is due to oxygen that lowers the binding energy of hydrogen on the (110) surface (**Figure 11**). It consequently lowers the activation barrier for recombination and make the process faster, while it decreases at the same time the total amount of hydrogen on the surface.

### 5.3 – Summary on absorption desorption at saturation and over.

From the energy profiles displayed in **Figure 13**, tungsten displays three distinct zones: the surface at coordinate 0, the sub-surface up to Td<sub>4</sub>, and the bulk below. The surface is the point of lowest energy for hydrogen, and the sub-surface shows a highly distorted energy profile for hydrogen diffusion.

Regarding the absorption of hydrogen, we distinguished between mechanisms at surface *saturation* and *oversaturation*. *Oversaturation* dramatically lowers the activation barriers for absorption into the bulk and recombination on the surface.

In any case, oxygen lowers the binding energy of hydrogen to the surface, which decreases the activation barrier from  $\theta_o = 0.0$  to  $\theta_o = 0.50$ . This result is supported by experimental evidence: (i) Dunand et al. [26] show a shift in the TDS peak from 415K to 380K with increasing O coverage. Also Whitten and Gomer [25] measured a heat of desorption for hydrogen of 1.00 eV and 1.21eV at low and high coverage in oxygen. This is in excellent agreement with the heat of desorption we computed here for hydrogen at 0.94eV and 1.24eV for coverages  $\theta_o = 0.25$  and  $\theta_o = 0.50$  at surface *saturation*.

## 6. Discussion and Conclusion

In the present paper, we first investigated by DFT the stable adsorption site for oxygen on the (110) surface of tungsten up to saturation and beyond. The adsorption patterns were determined

in good agreement with previous LEED measurements. The diffusion properties of oxygen on the surface were also determined: the activation barrier increases as the oxygen coverage increases. Above saturation in oxygen, it is shown that tungsten oxide  $\text{WO}_2$  may form, but due to the diversity of the mechanisms involved, no conclusion is drawn with regard to this point. The co-adsorption of hydrogen and oxygen is further investigated. It is shown that both hydrogen and oxygen adsorb at TF sites. The saturation limit of the surface was determined at one monolayer in adsorbate. This implies that oxygen, once adsorbed, limits the amount of hydrogen that adsorbs on the surface. This finding is in good agreement with experimental measurements by TDS [25,26]. In addition, the presence of oxygen on the W(110) surface lowers the binding energy of hydrogen, which is also consistent with TDS measurements [25,26].

The absorption and release mechanisms of hydrogen isotopes across the (110) surface of tungsten were already determined on the clean surface at  $\theta_o = 0.00$ . The impact of oxygen is here investigated at  $\theta_o = 0.25$  and  $\theta_o = 0.50$ : at *saturation* of the surface, the activation barrier for hydrogen absorption into the bulk is around 1.76 -1.77eV for both oxygen coverages, which is identical to the value on the clean surface. At *oversaturation* in adsorbate, absorption is made much faster since the activation barrier drops to 1.08 eV. The specific effect of oxygen manifests itself during the recombination process. As oxygen lowers the binding energy of hydrogen on the surface, it lowers the activation barrier for hydrogen recombination which kinetically activates this process.

Up to *saturation*, the activation energies for recombination are around one eV depending on the oxygen coverage. This is in the range of hydrogen detrapping from vacancies [35], which makes recombination among the rate-limiting steps of the kinetic of hydrogen release from tungsten. At *oversaturation*, the activation energy for recombination falls way below one eV at 0.59eV.

Recombination is no more the rate-limiting step, and no impact of the surface is expected on the global desorption mechanism of hydrogen from tungsten.

The present DFT model will be brought in the macroscopic rate equations code MHIMS to determine whether *oversaturation* in adsorbate of the surface is reached or not. This is a dynamical property that involves a balance between the flux from the bulk to the surface and the speed of recombination during desorption (conversely between the flux of hydrogen to the surface and the flux from the surface to the bulk). These dynamic properties will be investigated in a subsequent work with rate equations involving hydrogen flux balance at the surface.

## Acknowledgement

*This work has been carried out within the framework of the French Federation for Magnetic Fusion Studies (FR-FCM) and of the EUROfusion Consortium, funded by the European Union via the Euratom Research and Training Program (Grant Agreement No 101052200 — EUROfusion). Views and opinions expressed are however those of the author(s) only and do not necessarily reflect those of the European Union or the European Commission. Neither the European Union nor the European Commission can be held responsible for them. This work also received fund within the framework of the A\*MIDEX project (Grant No. ANR-11-IDEX-0001-02) funded by the Investissements d'Avenir French Government program, managed by the French National Research agency. The views and opinions expressed herein do not necessarily reflect those of the European Commission. The authors of this paper were granted access to the high-performance computing resources of IDRIS and CINES under Allocation No. A 0100806612 made by Grand Equipement National de Calcul Intensif and to the Marconi Supercomputer at CINECA Super Computing Application and Innovation Department, Bologna, Italy.*

## Bibliography

- [1] Loarte A, Lipschultz B, Kukushkin A S, Matthews G F, Stangeby P C, Asakura N, Counsell G F, G. Federici, Kallenbach A, Krieger K, Mahdavi A, Philipps V, Reiter D, Roth J, Strachan J, Whyte D, R. Doerner, Eich T, Fundamenski W, Herrmann A, Fenstermacher M, Ghendrih P, Groth M, Kirschner A, S. Konoshima, LaBombard B, Lang P, Leonard A W, Monier-Garbet P, Neu R, Pacher H, Pegourie B, R.A. Pitts, Takamura S, Terry J, Tsitron E, Layer the I S and Group D P T 2007 Chapter 4: Power and particle control Nucl. Fusion 47 S203.
- [2] Brezinsek S, Coenen J W, Schwarz-Selinger T, Schmid K, Kirschner A, Hakola A, Tabares F L, Meiden H J van der, Mayoral M-L, Reinhart M, Tsitron E, Ahlgren T, Aints M, Airila M, Almaviva S, E. Alves, Angot T, Anita V, Parra R A, Aumayr F, Balden M, Bauer J, Yaala M B, Berger B M, R. Bisson, Björkas C, Radovic I B, Borodin D, Bucalossi J, Butikova J, Butoi B, Čadež I, R. Caniello, Caneve L, Cartry G, Catarino N, Čekada M, Ciralo G, Ciupinski L,

- Colao F, Corre Y, C. Costin, Craciunescu T, Cremona A, Angeli M D, Castro A de, Dejarnac R, Dellasega D, Dinca P, T. Dittmar, Dobrea C, Hansen P, Drenik A, Eich T, Elgeti S, Falie D, Fedorczak N, Ferro Y, Fornal T, E. Fortuna-Zalesna, Gao L, Gasior P, Gherendi M, Ghezzi F, Gosar Ž, Greuner H, Grigore E, Grisolia C, M. Groth, Gruca M, Grzonka J, Gunn J P, Hassouni K, Heinola K, Höschen T, Huber S, Jacob W, Jepsu I, X. Jiang, Jogi I, Kaiser A, Karhunen J, Kelemen M, Köppen M, Koslowski H R, Kreter A, Kubkowska M, M. Laan, Laguardia L, Lahtinen A, Lasa A, Lazic V, Lemahieu N, Likonen J, Linke J, Litnovsky A, Ch. Linsmeier, Loewenhoff T, et al 2017 Plasma–wall interaction studies within the EUROfusion consortium: progress on plasma-facing components development and qualification Nucl. Fusion 57 116041
- [3] Grisolia C 1999 Plasma wall interaction during long pulse operation in Tore Supra Journal of Nuclear Materials 266–269 146–52.
- [4] J. Denis, J. Bucalossi, G. Ciraolo, E.A. Hodille, B. Pégourié, H. Bufferand, C. Grisolia, T. Loarer, Y. Marandet, E. Serre, JET Contributors, Nuclear Materials and Energy, 19 (2019) 550-557, Dynamic modelling of local fuel inventory and desorption in the whole tokamak vacuum-vessel for auto-consistent plasma-wall interaction simulations.
- [5] E.A. Hodille, A. Založnik, S. Markelj, T. Schwarz-Selinger, C.S. Becquart, R. Bisson and C. Grisolia, Nuclear Fusion 57 (2017) 056002.
- [6] A. Založnik, S. Markelj, T. Schwarz-Selinger, K. Schmid, Deuterium atom loading of self damaged tungsten at different sample temperatures, JNM 496 (2017) 1-8
- [7] E.A. Hodille, S. Markelj, M. Pecovnik, M Ajmalghan, Z.A. Piazza, Y. Ferro, T. Schwarz-Selinger and C. Grisolia, Nuclear Fusion 60 (2020) 106011, Kinetic model for hydrogen absorption in tungsten with coverage dependent surface mechanisms.
- [8] E. A. Hodille, M. Payet, V. Marascu, S. Peillon, J. Mougnot, Y. Ferro, R. Delaporte-Mathurin, F. Leblond, E. Bernard and C. Grisolia, Nuclear Fusion 61 (2021) 086030, Modelling tritium adsorption and desorption from tungsten dust particles with a surface kinetic model
- [9] Matveev D, Wensing M, Ferry L, Virof F, Barrachin M, Ferro Y and Linsmeier Ch, Nuclear Instruments and Methods in Physics Research Section B: Beam Interactions with Materials and Atoms 430 (2018) 23–30, Reaction-diffusion modeling of hydrogen transport and surface effects in application to single-crystalline Be.
- [10] K. Schmid and M. Zibrov, Nuclear Fusion, 61 (2021) 086008, On the Use of Recombination Rate Coefficients in Hydrogen Transport Calculations.
- [11] Z. A. Piazza, M. Ajmalghan, Y. Ferro and R. D. Kolasinski, Acta Materialia, 145 (2018) 388-398. Saturation of tungsten surfaces with hydrogen: a density functional theory study complemented by low energy ion scattering and direct recoil spectroscopy data.
- [12] Z. A. Piazza, R. D. Kolasinski, M. Ajmalghan, E. Hodille, Y. Ferro\* - Journal of Physical Chemistry C 125 (2021) 16086 – 16906, A predictive atomistic model for hydrogen adsorption on metal surfaces: comparison with low energy ion beam analysis on tungsten.
- [13] Z. J. Bergstrom, C. Li, G. D. Samolyuk, B. P. Uberuaga, and B.D. Wirth, J. Phys.:Condens. Matter, 31 (2019) 255002, Hydrogen interaction with low index surface orientations of tungsten.
- [14] Z. A. Piazza, M. Ajmalghan, R. D. Kolasinski and Y. Ferro, Physica Scripta, T171 (2020) 014025, A density functional theory based thermodynamic model of hydrogen coverage on the W(110) surface.
- [15] A. Nojima, K. Yamashita, Surf. Sci. 601 (2007) 3003–3011, A theoretical study of



hydrogen adsorption and diffusion on a W(110) surface.

[16] K. Heinola, T. Ahlgren, Phys. Rev. B. 81 (2010) 073409, First-principles study of H on the reconstructed W(100) surface.

[17] M. Ajmalghan, Z. A. Piazza, E. Hodille, Y. Ferro - Nuclear Fusion 59 (2019) 106022 Surface coverage dependent mechanisms for the absorption and desorption of hydrogen from the W(110) and W(100) surfaces: a DFT investigation.

[18] L. Yang, and B. D. Wirth, Journal of Applied Physics, 125 (2019) 165105, first-principles study of hydrogen diffusion and self-clustering below tungsten surfaces.

[19] D.F. Johnson, E.A. Carter, J. Mater. Res. 25 (2010) 315–327, Hydrogen in tungsten: Absorption, diffusion, vacancy trapping, and decohesion.

[20] A. Moitra, K. Solanki, Comput. Mater. Sci. 50 (2011) 2291–2294, Adsorption and penetration of hydrogen in W: A first principles study.

[21] L. Yang, and B. D. Wirth, Surface Sciences, 717 (2022) 121983, Boron segregation and effect on hydrogen energetics near tungsten surfaces: A first-principles study.

[22] A. Gallo et al Nucl. Fusion 60 (2020) 126048 Interpretative transport modeling of the WEST boundary plasma: main plasma and light impurities

[23] M Balden et al, Phys. Scr. 96 (2021) 124020 Erosion and redeposition patterns on entire erosion marker tiles after exposure in the first operation phase of WEST

[24] K. Kremer, M. Brucker, W. Jacob, T.Schwarz-Selinger, Nuclear Materials and Energy 30 (2022) 101137, Influence of thin oxide films on hydrogen isotope release from non-irradiated tungsten.

[25] J.E.Whitten, R. Gomer, Surface Sciences, 409 (1998) 16-26. The co-adsorption of H and O on the W(110) surface.

[26] A. Dunand, M. Minissale, J.-B. Faure, L. Gallais, T. Angot and R. Bisson. Nucl. Fusion 62 (2022) 054002, Surface oxygen versus native oxide on tungsten: contrasting effects on deuterium retention and release.

[27] M. Stöhr, R. Podloucky, and S. Müller, J. Phys.: Condens. Matter 21 (2009) 134107, Ab initio phase diagram of oxygen adsorption on W(110).

[28] E.A. Hodille, X. Bonnin, R. Bisson, T. Angot, C.S. Becquart, J.M. Layet, C. Grisolia, J. Nucl. Matter. 467 (2015) 424-431, Macroscopic rate equation modeling of trapping/detrapping of hydrogen isotopes in tungsten materials

[29] P. Giannozzi, S. Baroni, N. Bonini, M. Calandra, R. Car, C. Cavazzoni, D. Ceresoli, G. L. Chiarotti, M. Cococcioni, I. Dabo, A. Dal Corso, S. de Gironcoli, S. Fabris, G. Fratesi, R. Gebauer, U. Gerstmann, C. Gougoussis, A. Kokalj, M. Lazzeri, L. Martin-Samos, N. Marzari, F. Mauri, R. Mazzarello, S. Paolini, A. Pasquarello, L. Paulatto, C. Sbraccia, S. Scandolo, G. Sclauzero, A. P. Seitsonen, A. Smogunov, P. Umari, and R. M. Wentzcovitch, J. Phys.: Condens. Matter 21 (2009) 395502.

[30] J. P. Perdew, K. Burke, and M. Ernzerhof, Phys. Rev. Lett. 77 (1996) 3865.

[31] D. Vanderbilt, Phys. Rev. B 41 (1990) 7892.

[32] L. Wang, T. Maxisch, and G. Ceder, B 73 (2006) 195107, Oxidation energies of transition metal oxides within the GGA+U framework.

[33] B. Hammer, L. B. Hansen, J.K.Nørskov; Phys. Rev. B, 59 (1999) Improved adsorption energetics within density-functional theory using revised Perdew-Burke-Ernzerhof functionals.

- [34] J. A. Pople, M. H. Gordon, D. J. Fox, K. Raghavachari, and L. A. Curtiss, *J. Chem. Phys.* 90, (1989) 5622.
- [35] N. Fernandez, Y. Ferro, D. Kato, Hydrogen diffusion and vacancies formation in tungsten: Density Functional Theory calculations and statistical models, *Acta Materialia*. 94 (2015) 307–318.
- [36] N. Marzari, D. Vanderbilt, A. De Vita, M. Payne, *Phys. Rev. Lett.* 82 (1999) 3296.
- [37] G. Henkelman, B.P. Uberuaga, H. Johnsson, *J. Chem. Phys.* 113 (2000) 9901-9904. A climbing image nudged elastic band method for finding saddle points and minimum energy paths.
- [38], Baroni S, de Gironcoli S, Dal Corso A and Giannozzi P 2001 Phonons and related crystal properties from density-functional perturbation theory *Rev. Mod. Phys.* 73 515–62
- [39] K. E. Johnson, R. J. Wilson, and S. Chiang, *Phys. Rev. Lett.* 71 (1993) 1055-1058, Effects of Adsorption Site and Surface Stress on Ordered Structures of Oxygen Adsorbed on W(110)
- [40] J. R. Chen and R. Gomer, *Surf. Sci.* 79 (1979), 413-444, Mobility of oxygen on the W(110) plane of tungsten.
- [41] G.C. Wang, T.M. Lu, and M. G. Lagally, *J. Chem.Phys.* 69 (1978) 479, Phase transitions in the chemisorbed layer W(110) p(2×1)–O as a function of coverage. I. Experimental.
- [42] M. A. Van Hove and S. Y. Tong, *Phys. Rev. Lett.* 35 (1975) 1092, Chemisorption Bond Length and Binding Location of Oxygen in a p(2×1) Overlayer on W(110) Using a Convergent, Perturbative, Low-Energy-Electron-Diffraction Calculation.
- [43] R. Butz and H. Wagner, *Surf. Sci* 63 (1977) 448-459, Diffusion of oxygen on tungsten (110)
- [44] C. Uebing, R. Gomer 381 (1997) 33-48, The diffusion of oxygen on W(110), the influence of the p(2×1) ordering.
- [45] H. Daimon, R. Ynzunza, J. Palomares, H. Takabi, and C. S. Fadely, *Surf. Sci.* 408 (1998) 260-267, direct structure analysis of W(110)-p(1×1) by full solid-angle X-ray photoelectron diffraction with electrochemical-state resolution.
- [46] R. Ynzunza, J. Palomares, E. D. Tober, Z. Wang, J. Morais, R. Denecke, H. Daimon, Y. Chen, Z. Hussain, M. A. Van Hove, and C. S. Fadely, *Surf. Sci.* 442 (1999) 27-35, Structure determination for saturated p(1×1) oxygen on W(110) from full solid angle photoelectron diffraction with chemical-state resolution.
- [47] C.Kohrt and R. Gomer, *J. Chem. Phys* 52 (1970) 3283, Adsorption of Oxygen on the (110) plane of tungsten.
- [48] A. Szabo and N. S. Ostlund, *Modern Quantum Chemistry, Introduction to advanced structure theory*, McGraw-Hill Publishing Compagny 1989, pp 151-152.